Available online at www.sciencedirect.com
SCIENCE DIRECT
Materials Research Bulletin 41 (2006) 714–723
Materials Research Bulletin
www.elsevier.com/locate/matresbu

Kinetic study of $ZnFe_2O_4$ formation from mechanochemically activated Zn–Fe_2O_3 mixtures

P.M. Botta [a,*], E.F. Aglietti [b], J.M. Porto López [a]

[a] *Instituto de Investigaciones en Ciencia y Tecnología de Materiales (INTEMA), J.B. Justo 4302, B7608FDQ Mar del Plata, Argentina*
[b] *Centro de Tecnología de Recursos Minerales y Cerámica (CETMIC), Camino P. Centenario y 506, 1897 M.B. Gonnet, Argentina*

Received 18 January 2005; received in revised form 26 September 2005; accepted 10 October 2005
Available online 2 November 2005

Abstract

The kinetics of $ZnFe_2O_4$ formation starting from mechanochemically activated Zn–Fe_2O_3 powders are studied. Mixtures of metallic Zn and hematite were activated under air atmosphere in a high energy mill and thermally treated at temperatures between 500 and 650 °C during several holding times. During the activation, morphological and compositional changes were observed, but $ZnFe_2O_4$ formation was not detected. The $ZnFe_2O_4$ content in heated samples was determined using quantitative X-ray diffraction analysis. The resulting conversion–time curves were fitted using different kinetic models of solid-state reaction, calculating the kinetic parameters of the studied reaction. The comparison with the conventional synthesis method revealed that the mechanochemical treatment provoked a change of the rate-controlling step and a significant decrease of the activation energy, which was more evident for the more activated mixtures.

Keywords: A. Ceramics; C. X-ray diffraction; D. Diffusion

1. Introduction

Soft magnetic ferrites with spinel structure are materials with many applications in electronic and telecommunication industries. This applicability is based on the combination of three fundamental characteristics: high electrical resistivity, wide range of magnetic properties (which are strongly dependent on the cation distribution) and relative simplicity of fabrication through conventional techniques [1,2].

The conventional synthesis of spinel ferrites starts from elemental oxide powders mixtures, which are milled, formed and finally sintered at temperatures above 1300 °C. Conventionally prepared $ZnFe_2O_4$ is a normal spinel, whose tetrahedral and octahedral sites are partially occupied by Zn^{2+} and Fe^{3+} cations, respectively. In spite of this cation distribution and the electronic configuration of both cations (which should produce an antiferromagnetic behavior) this ferrite is paramagnetic at room temperature. However, it is a well-known fact that this behavior is strongly dependent of the synthesis and processing conditions [3,4]. In fact, uncommonly high magnetization has been measured in $ZnFe_2O_4$ ultrathin particles [5]. This anomalous behavior has recently led to investigate alternative

* Corresponding author.

0025-5408/$ – see front matter © 2005 Elsevier Ltd. All rights reserved.
doi:10.1016/j.materresbull.2005.10.011

synthesis methods for ferrites, such as sol–gel [6], coprecipitation [7], hydrothermal synthesis [8], etc., aiming to the formation of nanoparticles, which might increase the field of applications of these materials. There are other applications of $ZnFe_2O_4$ that do not exploit its magnetic properties, such as its use as desulfurating agent of synthesis gas [9] and, in recent years, the possibility of using zinc ferrite as a NO sensor in exhaust gases [10].

In the last 20 years, mechanochemical activation has become a very useful technique to synthesize a great variety of materials [11,12]. The method is particularly attractive for preparing metastable phases or materials whose properties are dependent on its ion distribution, such as $ZnFe_2O_4$. Moreover, from an operative point of view the mechanochemical technique is more advantageous than the wet-route methods, since it is easier to control and does not require the use of expensive and labile reactants. In spite of these advantages of the mechanochemical method, a limited understanding of the phenomena involved during the activation is often recognized as one of their most important limitations [13]. Surprisingly, there are few investigations concerning the effects of mechanochemical treatments on the kinetics of solid-state reactions. Some works have focused on reactions between metals [14], phase transformations of inorganic oxides [15] and metal oxide reactions [16]. Recently, a kinetic study of crystallization of $ZnFe_2O_4$ starting from an activated mixture of iron and zinc oxide was reported [17]. However, investigations including the determination of activation energies and mechanisms of chemical reactions as a function of milling time are still lacking. These studies can be interesting for its potential application in the control of solid-state reactions as well as for its contribution to the understanding of the mechanochemical phenomena in inorganic solids.

In this work, a new route to synthesize $ZnFe_2O_4$ starting from Fe_2O_3 and metallic Zn is proposed. The use of Zn instead of ZnO has demonstrated to be effective to prepare this and other mixed oxides [18,19]. In this way, this paper has a double purpose: on one hand, to establish a simple methodology for preparing zinc ferrite through less severe experimental conditions, and on the other hand, to contribute to the understanding of the effects of mechanochemical treatments on the kinetics of solid-state reactions.

2. Materials and methods

2.1. Mechanical activation

The reactive mixture was prepared starting from metallic Zn powder (commercial reagent, 99.0 wt.%) and hematite (commercial reagent, 98.5 wt.% of Fe_2O_3) in molar ratio 1:1. The mixture was mechanically activated in a Herzog HSM100 vibrating mill. This equipment consists of a 200 cm^3 Cr-steel milling chamber, which was loaded with 60 g of reactive powder, a cylinder and a concentric ring (both made of Cr-steel), resulting in a milling media-to-powder mass ratio of about 60. The chamber was put under planetary movement (12.5 Hz) during times up to 30 min. At 6 and 18 min, small portions (about 2 g) were withdrawn from the mill. The obtained samples were named ZH*x*, where *x* is the activation time in minutes.

The phase evolution of the activated mixtures was determined by X-ray diffraction (XRD), using a Philips PW1830/00 diffractometer with Co Kα radiation at 40 kV and 30 mA. Crystallite size (D_c) and microstrain ($\langle \varepsilon^2 \rangle^{1/2}$) of hematite particles were estimated for each sample. The breadth method [20] was used after a Voigt deconvolution of the peak of maximum intensity ($d = 0.2700$ nm). This single-line method is based on the assumption that the lattice disorder exhibits a Gaussian distribution, whereas the peak broadening follows a Cauchy profile. A silicon pattern was used to determine the instrumental width. In order to select adequate reaction temperatures, differential and gravimetric thermal analyses (DTA and TGA) were carried out in a Shimadzu DTA/TGA-50H instrument, using a sample mass of 40 mg and a heating rate of 10 °C/min under flowing air.

2.2. Thermal treatments

The samples ZH6, ZH18 and ZH30 were submitted to thermal treatments in an electric furnace at 500, 575 and 650 °C, during times between 2 min and 24 h, depending on activation times and heating temperatures. In each sample, the $ZnFe_2O_4$ content was determined by XRD using the external standard method [21]. The peak selected for the analysis is located at $d = 0.2543$ nm ($2\theta = 41.22°$, using Co Kα radiation). The choice of this signal was based on its high relative intensity and non-overlapping with other peaks. The $ZnFe_2O_4$ standard was prepared by thermal treatment at 700 °C for 2 h of a Zn–Fe_2O_3 powder mixture, which was previously mechanically activated for 18 min.

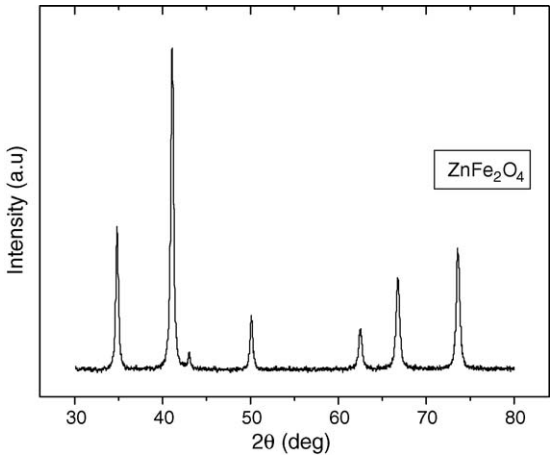

Fig. 1. XRD diagram of the $ZnFe_2O_4$ obtained pattern.

The relatively low temperature used for preparing the standard allows assuming a crystallinity similar to that of the $ZnFe_2O_4$ formed in the samples. In Fig. 1, the XRD diffractogram of the prepared standard is observed.

2.3. Application of kinetic models

Several kinetic models of solid-state reactions were tested in order to fit the obtained conversion–time curves [22]. Although the oldest models date from as long as 70 years ago, even nowadays some of them are used to describe most solid-state reactions. Basically, it is possible to classify them in three different types: models in which the product growth is controlled by diffusion reactants or diffusional models, models in which the controlling step is the chemical reaction at the interphase and models where the reaction rate is governed by nucleation-growth. Two diffusional models, developed by Jander and Dunwald–Wagner, were selected to test the experimental data. Also, the nucleation-growth and chemical reaction models were tested. Table 1 summarizes the mathematical functions that were tested for linear fit and the obtainable parameters for each proposed model. Through the linearized Arrhenius equation (Eq. (1)), the best fit was used to determine the activation energy (E_a) of $ZnFe_2O_4$ formation in each reactive mixture

$$\ln k = \ln A - \frac{E_a}{RT}, \tag{1}$$

where k is the reaction rate coefficient, A the pre-exponential factor, R the gases constant and T is the absolute temperature.

3. Results and discussion

Fig. 2 shows the XRD diagrams for the non-activated (ZH0) and activated mixtures (ZH6, ZH18 and ZH30). A fast decrease of the peak intensity for both reactant phases is observed. For hematite, this is a consequence of the loss of

Table 1
Kinetic models used for fitting experimental conversion–time curves

Model	Plotted function	Parameters
Jander	$[1-(1-\alpha)^{1/3}]^2$ vs. t	Slope = k_J
Dunwald–Wagner	$\ln\left(\frac{6}{\pi^2(1-\alpha)}\right)$ vs. t	Slope = k_{DW}
Chemical reaction	$[1-(1-\alpha)^{1/3}]^2$ vs. t	Slope = k_{CR}
Nucleation-growth	$\ln\left[\ln\left[\frac{1}{1-\alpha}\right]\right]$ vs. $\ln[t]$	Slope = m; intercept = $m \ln[k_N]$

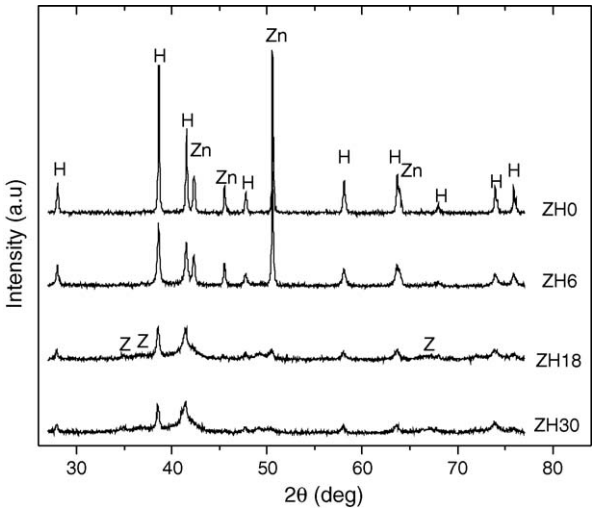

Fig. 2. XRD diagrams of ZH*x* samples. H: hematite (Fe_2O_3); Z: zincite (ZnO).

crystallinity provoked by accumulation of defects in the structure during the activation. For metallic zinc, this effect is the result of both the loss of crystallinity and the partial atmospheric oxidation, which seems to be significant from 18 min on. In fact, in the diffractogram of sample ZH18, weak and wide peaks of ZnO (zincite) can be noticed. Moreover, the diffracted signals of Zn show a clear widening with longer milling times, suggesting that the metal is plastically deformed during the mechanical treatment. According to recently published results, in a joint milling of two components, the particles of the more brittle phase tend to become covered by the more plastic phase [23]. In this way, it is possible that during the activation of the Zn–Fe_2O_3 mixture, the metal is deformed on the surface of the brittle hematite particles. This characteristic of the solid mixture was considered in order to select those diffusional kinetic models that agree with this morphological description of the reactive system.

Fig. 3 shows the crystallite size and microstrain for α-Fe_2O_3 as a function of activation time. Both parameters are expressed as relative changes to the respective values obtained for the non-activated mixture. According to the duration of the mechanochemical treatment, well-different effects are observed. At short times, the main effect is the fracture of the crystals, which undergo a size decrease of 90% in only 6 min of milling. However, at longer times the formation of microstrains becomes more significant, especially during the last 12 min of activation where an increase of 60% is observed.

The DTA and TGA traces of the prepared mixtures are shown in Fig. 4a and b, respectively. For samples ZH0 and ZH6, an endothermic peak corresponding to Zn melting is observed at 420 °C (Fig. 4a). In addition, an exothermic event with decreasing intensity and temperature can be noticed for all the samples. TGA curves (Fig. 4b) show a mass

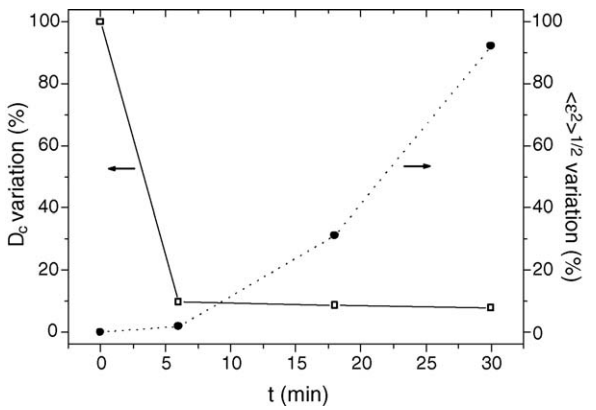

Fig. 3. Crystallite size (D_c) and microstrain ($\langle \varepsilon^2 \rangle^{1/2}$) for hematite as a function of milling time.

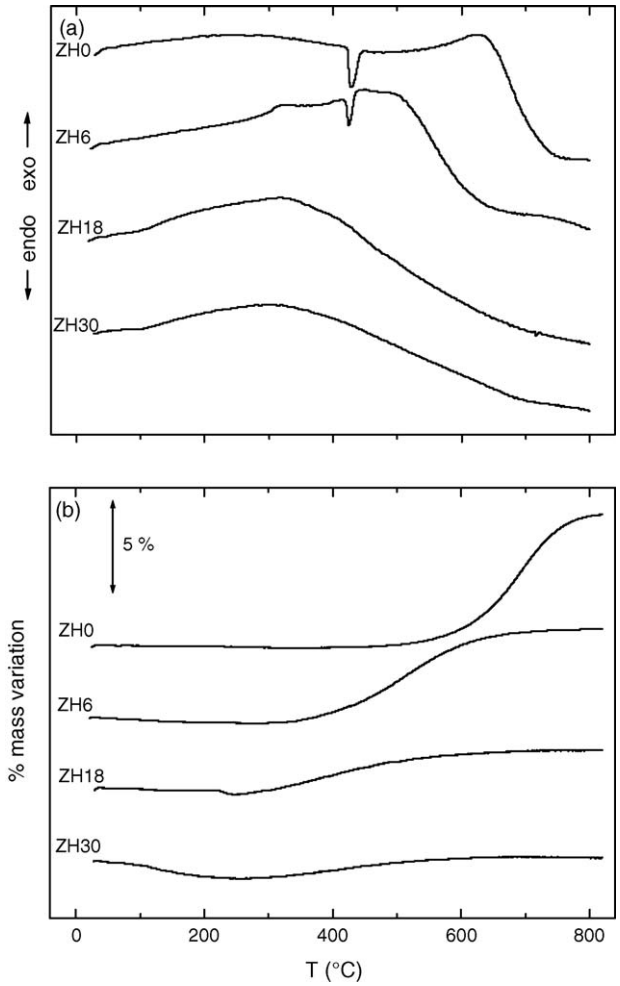

Fig. 4. Differential (a) and gravimetric (b) thermal analyses for ZH*x* samples.

gain, which is also shifted at lower temperatures for the more activated powders. For ZH0, this band appears at 650 °C, for ZH6 at 500 °C and for ZH18 and ZH30 it is observed approximately at 350 °C. This exothermic mass gain is attributed to the oxidation of metallic Zn, remaining from the mechanical activation. Taking into account these results, the mass percentage of Zn oxidized during the milling was calculated for each sample. The resulting values are presented in Table 2. An extensive oxidation of the metal at only 30 min of activation is observed.

Fig. 5a–c shows the conversion–time curves obtained for the activated mixtures heated at 500, 575 and 650 °C, respectively. A marked difference of reactivity between the sample ZH6 and the mixtures activated by 18 and 30 min is observed. ZH6 shows low conversion values even at the longest reaction times; these values vary from 0.25 at 500 °C to 0.60 at 650 °C. In contrast, samples ZH18 and ZH30 exhibit much higher conversion values and reaction rates. At 500 °C, $ZnFe_2O_4$ conversions reach 0.37 for ZH18 and 0.45 for ZH30; at 575 °C this value is about 0.65 for ZH18 and 0.75 for ZH30; at 650 °C both samples overcome a conversion of 0.80. In spite of these differences, the conversion–

Table 2
Percentages of oxidized Zn during the mechanical activation

Activation time (min)	Oxidized Zn (wt.%)
6	25
18	67
30	84

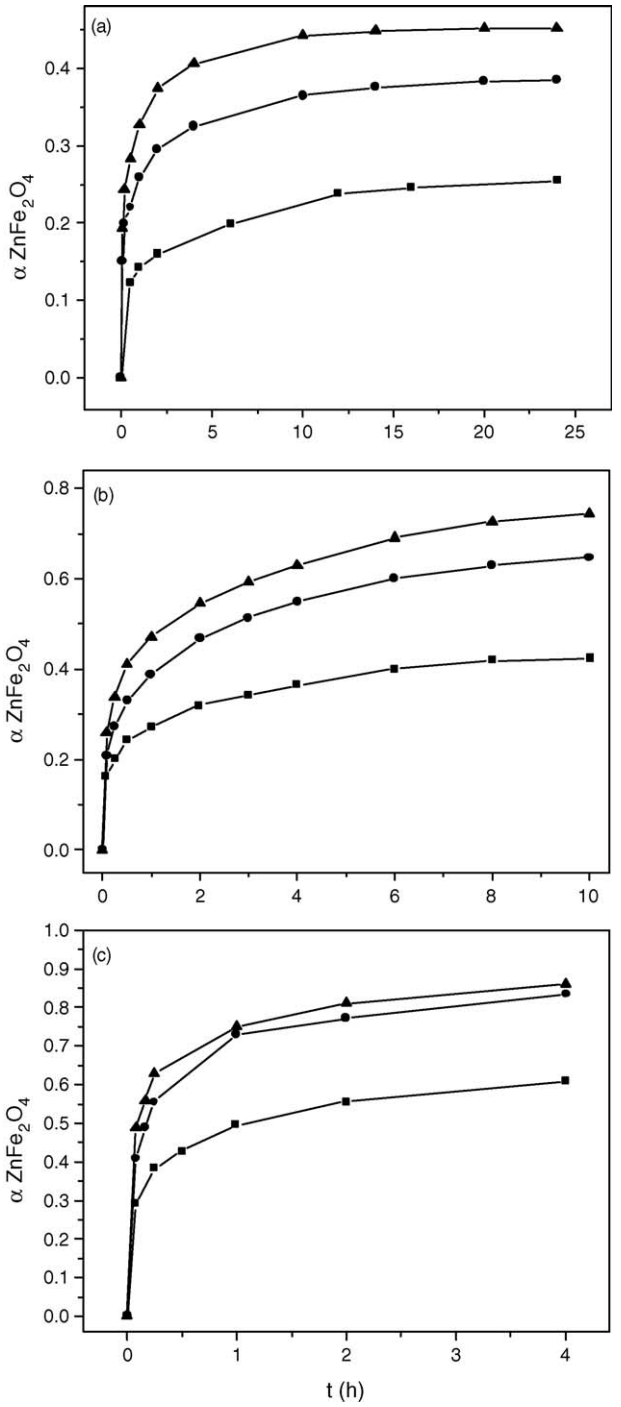

Fig. 5. Conversion–time curves obtained for the activated mixtures heated at: 500 °C (a), 575 °C (b) and 650 °C (c). (■) ZH6; (●) ZH18; (▲) ZH30.

time curves obtained for ZH18 and ZH30 show a similar behavior: both reach high conversion values at very short heating times and exhibit much slower reaction rates as $ZnFe_2O_4$ conversion increases. This steep increase of α at short heating times made difficult to apply the reduced time method [24] (in which the conversion is represented as a function of $t/t_{0.5}$, where $t_{0.5}$ is the time for $\alpha = 0.5$) in order to determine the appropriate kinetic model. Nevertheless, the method used here is completely equivalent, since it is based on the same classical kinetic models.

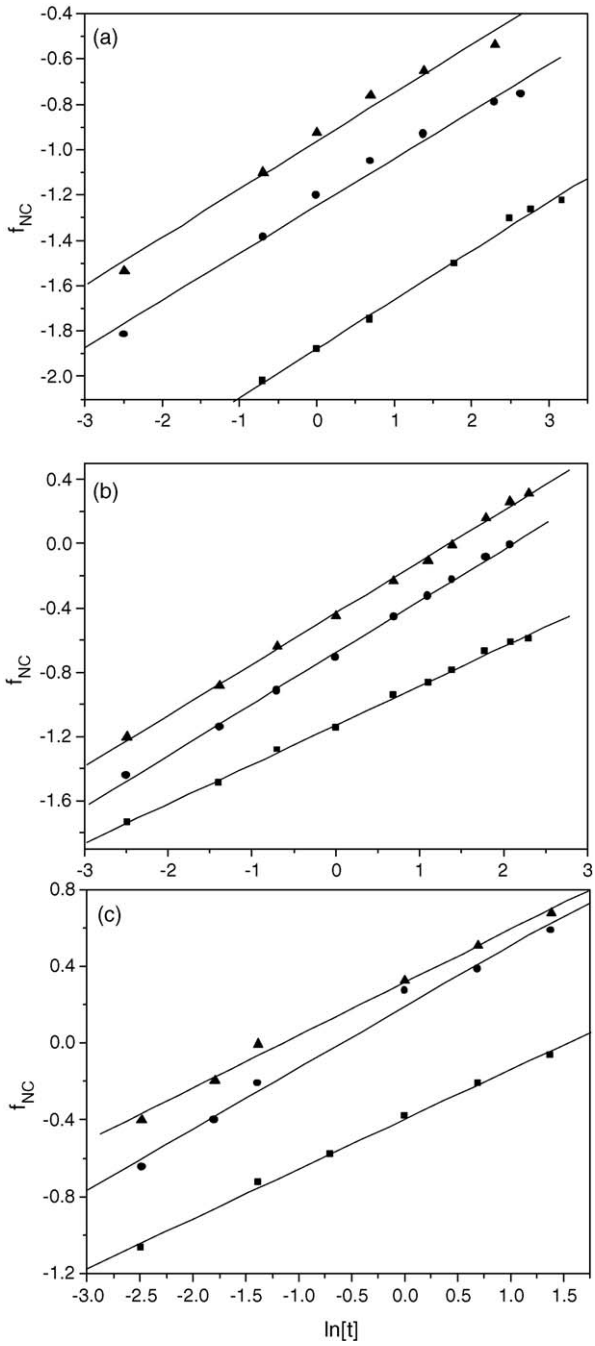

Fig. 6. Linear fit of the experimental data using the nucleation-growth model at: 500 °C (a), 575 °C (b) and 650 °C (c). (■) ZH6; (●) ZH18; (▲) ZH30.

In the case of ZH0, the conversion to $ZnFe_2O_4$ showed a steep increase with small temperature changes (for instance, the sample did not show any reaction after 24 h at 725 °C and reacted almost completely after a few minutes at 750 °C). For this reason, the determination of accurate time–conversion values was not possible.

For the activated mixtures the results of fitting each conversion–time curve with each theoretical model showed that the only linear fit was obtained applying the nucleation-growth model. With the other tested models, logarithmic-type curves were obtained instead of straight lines. This indicates that these kinetic models did not accurately describe the $ZnFe_2O_4$ formation from the studied Zn–Fe_2O_3 mixtures.

Table 3
Results of applying the nucleation-growth model to the kinetic data of the activated mixtures

Reactive mixture	Slope	Intercept	r	k_N (h^{-1})
$T = 500$ °C				
ZH6	0.216	−1.878	0.997	1.68×10^{-4}
ZH18	0.208	−1.248	0.993	2.48×10^{-3}
ZH30	0.213	−0.961	0.992	0.011
$T = 575$ °C				
ZH6	0.245	−1.132	0.999	9.85×10^{-3}
ZH18	0.321	−0.679	0.999	0.120
ZH30	0.319	−0.432	0.999	0.259
$T = 650$ °C				
ZH6	0.259	−0.397	0.998	0.216
ZH18	0.318	0.189	0.995	1.811
ZH30	0.275	0.316	0.997	3.158

Fig. 6a–c shows the plots corresponding to nucleation-growth model for the three activated samples heated at 500, 575 and 650 °C, respectively. In all the cases a good linear fit is observed, with regression coefficients (r) very close to 1. Table 3 displays the parameters obtained from the fitted lines, and the rate coefficient values (k_N) calculated from them. The analysis at constant temperature of these coefficients reveals that they increase significantly with the activation degree. The most important differences are observed between ZH6 and ZH18, while the rate coefficients obtained for ZH18 and ZH30 are clearly closer. The increment of the thermal treatment temperature produces an approach of k_N values obtained for each activation time. At 575 °C, the rate coefficient for ZH30 doubles the corresponding to ZH18, and this value is in its turn 12 times higher than k_N of ZH6. All these ratios are smaller at 650 °C: between ZH30 and ZH18 the ratio is only 1.7, whereas between ZH18 and ZH6 it is approximately 8.

Fig. 7 is an Arrhenius graph, where $\ln[k_N]$ is plotted versus T^{-1} for the three activated samples. A linear fitting allows obtaining the activation energy of the reaction, whose values are shown in Table 4. The calculated E_a values for all the samples are in good agreement with those previously reported for a conventional ceramic system, in which a reactive mixture of ZnO and Fe_2O_3 is heated at temperatures between 690 and 760 °C [25]. In these conditions, it is found that the reaction of $ZnFe_2O_4$ formation was governed by ionic diffusion, with an activation energy of 300 kJ/mol. In contrast, for the mechanochemically treated mixtures, the ionic diffusion is not the controlling step of the reaction kinetics, since the tested diffusional theoretical models did not adequately fit the experimental conversion–

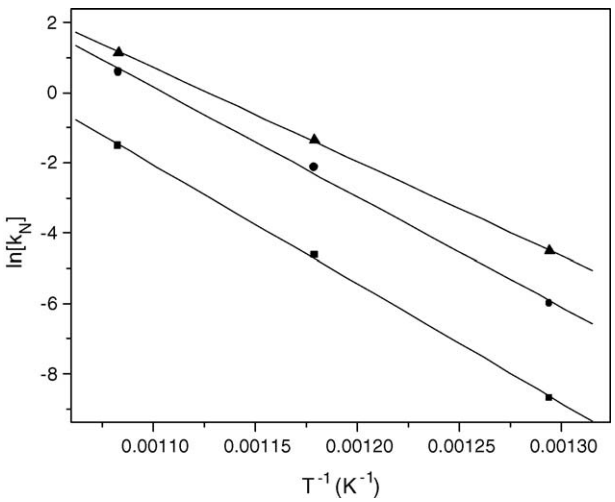

Fig. 7. Linear fit of Arrhenius equation for the three activated mixtures. (■) ZH6; (●) ZH18; (▲) ZH30.

Table 4
Kinetic parameters obtained from Fig. 3 for the mechanically activated mixtures

Sample	Slope (K)	Intercept	r	E_a (kJ/mol)
ZH6	−33981	35.3	−1.000	282.5
ZH18	−31332	34.6	−0.999	260.5
ZH30	−26846	30.3	−1.000	223.2

time curves. This suggests that the mechanical activation increases the ionic diffusion rate. Yang et al. report the same observation for a similar system [17]. They found an E_a value much lower than that obtained by us and also by Bamford et al., but it should be noted that this energy corresponds to the energy of $ZnFe_2O_4$ crystallization in a solid mixture already reacted during the mechanical treatment. In our study, the energy provided by the mechanical treatment is not enough to produce reaction during the activation. The creation of structural defects could give rise to a faster movement of the ions throughout the solid rather than the nucleation of a new phase ($ZnFe_2O_4$), changing the rate-controlling step of the reaction. An explanation for this observation could be the noticeable difference between crystalline structures of the Fe_2O_3 (hexagonal) and the nuclei of $ZnFe_2O_4$ (cubic), which have to form and grow in an unlike matrix. Taking into account that Zn^{2+} cations are the most mobile of the system [25], the ferrite formation requires the diffusion of these ions through the Fe_2O_3 structure such as the reticular rearrangement that may possible the formation of the cubic spinel phase.

The comparison of activation energies obtained for the milled mixtures reveals a significant decrease of this kinetic parameter as the mechanical treatment time is longer. Between the mixtures activated during 6 and 30 min a variation of 21% is registered. The marked increase of microstrains observed in this time range (Fig. 3) indicates a significant structural distortion of this oxide. This result suggests that the mechanochemical treatment produced not only an important increment of the ionic diffusion rate, but also enough structural distortion of hematite that could make easier the nucleation of zinc ferrite.

4. Conclusions

The mechanochemical treatment of Zn–Fe_2O_3 mixtures produced the amorphization of crystalline structures of the reactants, the deformation of metallic zinc and its almost complete oxidation after 30 min of milling.

During the thermal treatment, the formation rate of $ZnFe_2O_4$ was significantly increased by the previous mechanical treatment, reaching high conversions at temperatures lower than those used in conventional synthesis methods.

For the activated powder mixtures, the formation of $ZnFe_2O_4$ is governed by the nucleation and growth of the product phase, unlike the diffusional control reported for the conventional system.

The mixtures mechanically activated for 30 min showed a decrease of the activation energy for $ZnFe_2O_4$ formation of 21% with regard to the mixture activated for 6 min. This important variation can be explained on the basis of the deformation of the Fe_2O_3 crystalline structure, which makes possible a faster nucleation of a very different structure, such as $ZnFe_2O_4$.

Acknowledgements

The authors thank UNMdP, CONICET, ANPCyT and CIC for the financial support given to this work.

References

[1] M. Sugimoto, J. Am. Ceram. Soc. 82 (1999) 269.
[2] J. Smit, H.P.J. Wijn, Ferrites, J. Wiley & Sons, Amsterdam, 1959, p. 136.
[3] Yu.T. Pavljukhin, Ya.Ya. Medikov, V.V. Boldyrev, Mater. Res. Bull. 18 (1983) 1317–1327.
[4] V. Sepelák, K. Tkácová, V.V. Boldyrev, S. Wißmann, K.D. Becker, Physica B 234–236 (1997) 617.
[5] T. Kamiyama, H. Haneda, T. Sato, S. Ikeda, H. Asano, Solid State Commun. 81 (1992) 563–566.
[6] A. Chatterjee, D. Das, D. Pradhan, D. Chakravorty, J. Magn. Magn. Mater. 127 (1993) 214–218.

[7] J.L. Martin de Vidales, A. López-Delgado, E. Vila, F.A. López, J. Alloys Compd. 287 (1999) 276–283.
[8] S. Yu, F. Takahiro, Y. Masahiro, J. Magn. Magn. Mater. 256 (2003) 420–424.
[9] P. Druska, U. Steinike, V. Šepelák, J. Solid State Chem. 146 (1999) 13–21.
[10] N. Miura, S. Zhuiykhov, T. Ono, M. Hasei, N. Yamazoe, Sens. Actuators B 83 (2002) 222–229.
[11] K. Tkácová, in: D.W. Fuerstenau (Ed.), Developments in Mineral Processing, vol. 11, Elsevier, Amsterdam, 1989.
[12] D.L. Zhang, Prog. Mater. Sci. 49 (2004) 537–560.
[13] C. Suryanarayana, E. Ivanov, V.V. Boldyrev, Mater. Sci. Eng. A 304–306 (2001) 151–158.
[14] B.J.M. Aikin, T.H. Courtney, D.R. Maurice, Mater. Sci. Eng. A 147 (1991) 229–237.
[15] S. Begin-Colin, T. Girot, G. Le Caër, A. Mocellin, J. Solid State Chem. 149 (2000) 41–48.
[16] J.S. Forrester, G.B. Schaffer, Metall. Trans. A 26 (1995) 725–730.
[17] H. Yang, X. Zhang, C. Huang, W. Yang, G. Qiu, J. Phys. Chem. Solids 65 (2004) 1329–1332.
[18] P.M. Botta, P.G. Bercoff, E.F. Aglietti, H.R. Bertorello, J.M. Porto López, Mater. Sci. Eng. A 360 (2003) 146–152.
[19] P.M. Botta, E.F. Aglietti, J.M. Porto López, J. Mater. Sci. 39 (2004) 5195–5199.
[20] T.H. De Keijser, J.I. Langford, E.J. Mittemeijer, A.B.P. Vogels, J. Appl. Cryst. 15 (1982) 308–314.
[21] B.D. Cullity, Elements of X-Ray Diffraction, second ed., Addison-Wesley Publ. Co., Reading, 1976.
[22] S.F. Hulbert, J. Br. Ceram. Soc. 6 (1969) 11–20.
[23] N. Lyakhov, in: Proceedings of the Fourth International Conference in Mechanochemistry and Mechanical Alloying (INCOME 2003), 2004, p. 14.
[24] J.D. Hancock, J.H. Sharp, J. Am. Ceram. Soc. 55 (1972) 74–77.
[25] C.H. Bamford, C.F.H. Tipper, Comprehensive Chemical Kinetics, vol. 22, Elsevier, Amsterdam, 1980.